Dalton Transactions

ROYAL SOCIETY OF CHEMISTRY

PAPER

View Article Online
View Journal | View Issue

Cite this: *Dalton Trans.*, 2024, **53**, 9323

Synthesis and characterization of Pt(II) and Au(I) complexes with *N*-oxy-heterocyclic carbene ligands (NOHCs)†

Alice Benin,[a,b] Joshua Immanuel Kollar,[b] Tim Riesebeck,[b] Felix Wurl,[b] Claudia Graiff,[c] Thomas Strassner *[b] and Cristina Tubaro *[a]

Received 4th April 2024,
Accepted 25th April 2024

DOI: 10.1039/d4dt00996g

rsc.li/dalton

Two *N*-alkyloxy-*N*′-phenylimidazolium proligands and the corresponding platinum(II) cyclometalated *N*-alkyloxyimidazol-2-ylidene complexes with β-diketonate auxiliary ligands, [(C_{NOHC}^C*)Pt(LnL)] (LnL = acetyacetonate (acac) or 1,3-bis(2,4,6-trimethylphenyl)-propane-1,3-dionato (mesacac)) were synthesized and fully characterized. In addition, a Au(I) monocarbene complex was synthesized, isolated and characterized. Solid-state structures of two cyclometalated platinum(II) NOHC complexes and the Au(I) NOHC complex were obtained providing structural proof.

Introduction

In the last decade of the 20th century, Arduengo published the crystal structure of the first free N-heterocyclic carbene (NHC), the 1,3-diadamantylimidazol-2-ylidene, isolated by deprotonation of the corresponding azolium chloride salt.[1] Since then, NHC species themselves and their corresponding metal complexes have been widely studied.[2–7] Surprisingly, *N*-alkyloxy heterocyclic carbenes (NOHCs) have not received the same attention.[8–16] The most interesting feature of these carbenes is the influence given to the overall aromatic system by the presence of one or two oxygen atoms, linked to the nitrogen atoms of the heterocyclic ring. The carbene carbon atom is reported to be more nucleophilic than those of common NHCs. In a recent paper by Schreiner *et al.* two imidazole-based carbenes with adamantyl or adamantyloxy substituents were compared: both the carbene carbon chemical shift in the ^{13}C NMR spectra, and the ^{77}Se NMR chemical shift of the corresponding selenourea derivative, confirmed a remarkable increase in the electron donor properties of the carbene when the adamantyloxy substituent was present.[11]

A limited number of metal complexes with NOHC ligands have been reported so far, in particular silver(I),[8,10,13,14] gold(I),[8,10] copper(I),[10] palladium(II),[9,13] nickel(II)[9] and rhodium(I)[8,12,13] complexes. Not many applications have been investigated for this type of metal complexes and do not strongly differ from those typical for NHC analogues: for example cytotoxicity against colorectal cancer, promyelocytic leukaemia and breast cancer cell lines was reported for the Au(I) and Ag(I) benzyloxy NOHC complexes.[10]

To the best of our knowledge, no examples of cyclometalated NOHC (C_{NOHC}^C*) platinum(II) complexes have previously been reported in the peer-reviewed literature, although they have been briefly mentioned in a patent for Organic Light Emitting Diodes (OLEDs).[17] This is surprising considering that also several platinum(II) complexes with cyclometalated NHC ligands (C_{NHC}^C*) displayed interesting emitting properties for OLED applications.[18–25]

Herein, we report cyclometalated platinum(II) complexes with NOHC ligands, which were fully characterized by standard techniques. Additionally, UV/Vis, photoluminescence and electrochemical properties were investigated. A novel NOHC monocarbene gold(I) complex is also reported and confirmed by a solid-state structure.

Results

Synthesis and structural characterization of the complexes

The zwitterionic precursor **1** was synthesized adapting the procedure reported by Schreiner *et al.* for the analogous compound with the adamantyl substituent.[16] Diacetyl monoxime and hexahydro-1,3,5-triphenyltriazine were reacted in a 3 : 1 molar ratio in glacial acetic acid at room temperature

[a]*Dipartimento di Scienze Chimiche, Università di Padova, via Marzolo 1, 35131 Padova, Italy. E-mail: cristina.tubaro@unipd.it*
[b]*Physikalische Organische Chemie, Technische Universität Dresden, Bergstrasse 66, 01062 Dresden, Germany. E-mail: thomas.strassner@tu-dresden.de*
[c]*Dipartimento di Scienze Chimiche, della Vita e della Sostenibilità Ambientale, Università di Parma, Parco Area delle Scienze 17/A, 43124 Parma, Italy*

†Electronic supplementary information (ESI) available: NMR spectra, absorption and emission spectra, CVs and DPVs of the complexes, computational details. CCDC 2279855, 2279853 and 2279854. For ESI and crystallographic data in CIF or other electronic format see DOI: https://doi.org/10.1039/d4dt00996g

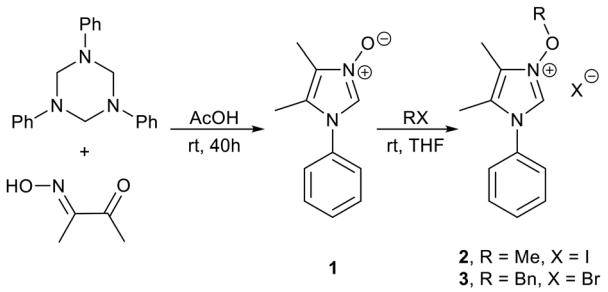

Scheme 1 Synthesis of the proligands **2** and **3**.

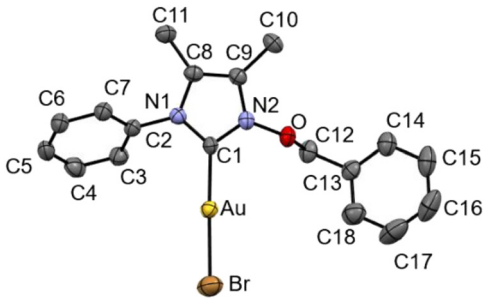

Fig. 1 ORTEP view of complex **4**. Ellipsoids are drawn at their 50% probability. Hydrogen atoms have been omitted for clarity. Selected bond distances (Å) and angles (°): Br–Au 2.365(1), Au–C1 1.975(5), C1–N1 1.353(6), C1–N2 1.345(8), C8–N1 1.401(8), C9–N2 1.384(8), N2–O 1.382(6), N1–C2 1.345(8); Br–Au–C1 178.4(2), N2–C1–N1 102.7(4), C12–O–N2 110.9(4).

for 40 h (Scheme 1). The proligands **2** and **3** were then obtained by mixing **1** with methyl iodide or benzyl bromide respectively, in anhydrous tetrahydrofuran in a pressure tube at room temperature.

The gold(I) complex **4** was synthesized starting from proligand **3** with a weak base assisted metalation, using K_2CO_3 as base (Scheme 2).[26,27] The formation of the complex was confirmed by the disappearance of the acidic C2–H signal at 10.65 ppm in the ^{1}H NMR spectrum (*cf.* ESI Fig. S7†). In addition, in the ^{13}C NMR spectrum the carbene carbon signal is located at 167.3 ppm (*cf.* ESI Fig. S8†). The mass spectrum of the complex presents a fragment at 753.2494 *m*/*z* which is attributable to the cationic bis(carbene) species $[Au(NOHC)_2]^+$, a species that can form in the presence of traces of water or under the measurement conditions.[28,29]

The proposed molecular structure of the complex was verified by single crystal X-ray diffraction analysis. In complex **4**, the gold centre has a linear coordination ($C_{carbene}$–Au–Br 178.4(2)°), as expected for a d^{10} metal centre (Fig. 1). The Au–$C_{carbene}$ (1.975(5) Å) and Au–Br (2.365(1) Å) distances are in agreement with the values reported in the literature for these bonds in complexes of the type (NHC)–Au–Br.[11] In contrast with the adamantyloxyimidazol-ylidene Au(I) complex reported by Schreiner, the C8–N1 and C9–N2 bond lengths do not differ significantly.[11]

The compound crystallizes in the $P2_1/n$ space group and the unit cell contains four molecules of the complex. Complexes are not superimposed, therefore the presence of aurophilic interactions can be excluded.

The synthesis of complexes **5**–**7** was achieved with the multi-step procedure, developed for the synthesis of analogous C^C* cyclometalated NHC platinum(II) complexes (Scheme 3).[30,31] The first step involves the *in situ* synthesis of the NHC–silver(I) complex by reaction of the azolium salts **2** or **3** with silver(I) oxide. Then the NHC ligand is transmetalated to platinum(II) and *ortho*-metalation of the phenyl ring is induced by heating the mixture. Finally, the auxiliary β-diketonato ligand is introduced. The acetylacetonate ligand (acac, R′ = Me) is added as sodium salt, while the 1,3-bis(2,4,6-trimethylphenyl)-propane-1,3-dionato ligand (mesacac, R′ = Mes) is generated *in situ* by deprotonation of the corresponding β-diketone with KO^{t}Bu.

The obtained Pt(II) complexes were fully characterized, including ^{1}H, ^{13}C and ^{195}Pt NMR spectra as well as high-resolution mass spectrometry. Successful cyclometalation was confirmed by the appearance of satellite peaks in the aromatic region (7.40–7.85 ppm) of the ^{1}H NMR spectra of the Pt(II) complexes due to the coupling with ^{195}Pt (*cf.* ESI Fig. S9, S15 and S17†).

In the ^{13}C NMR spectra, the carbene carbon signals can be observed in the range 144–146 ppm for the three Pt(II) complexes. The comparison between these results and those of analogous complexes,[30,31] having a metalated imidazole-2-ylidene with simple alkyl groups as nitrogen substituents, indi-

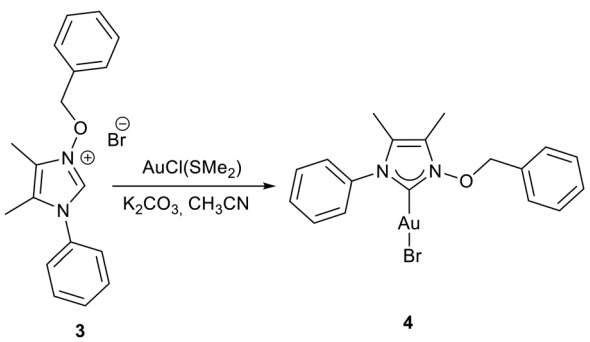

Scheme 2 Synthesis of complex **4** *via* weak base assisted metalation.

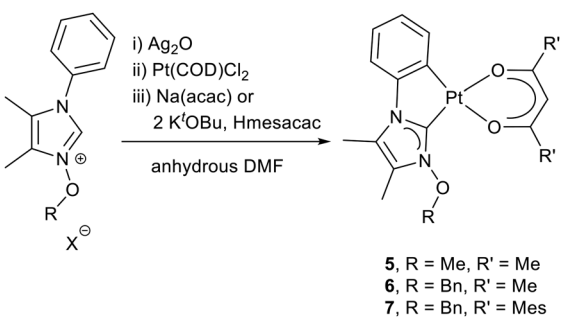

Scheme 3 Synthesis of the Pt(II) C^C* complexes **5**–**7**.

cates that no significant difference in the electron donation of the carbon atom towards the Pt(II) centre is observed by addition of the oxygen atom in the substituent structure.

Finally, the ^{195}Pt NMR signals are found at −3451, −3454 and −3398 ppm for **5**, **6** and **7**, respectively (*cf.* ESI Fig. S19†). These values are in accordance with values reported for C^C* Pt(II) complexes.[19,30] It is apparent that the Pt(II) centre in the mesacac compound **7** is less electron rich as its signal is shifted up field in comparison to the acac analogue **6**. The yields of the complexes are slightly lower than those of similar complexes with common imidazole-based carbenes. This could be related to the instability of the oxy-substituted compounds at high temperature.[8,32] On the contrary, the platinum (II) complexes are stable, in fact they melt without decomposition at considerably low temperatures, between 150 and 216 °C.

For complexes **5** and **7**, solid state structures were verified by X-ray diffractometry. Single crystals were grown by slow diffusion of pentane in concentrated dichloromethane solutions of the complexes. The X-ray structures of compounds **5** and **7** (Fig. 2 and 3) show a square planar geometry of the NOHC Pt(II) complexes. The angles C_{NOHC}–Pt–C* and O2–Pt–O3 were in fact 80.1(2) and 90.6(1)° for complex **5**, as well as 79.66(7) and 89.31(6)° for complex **7**. These values are comparable to those of analogous C^C* platinum(II) diketonate complexes.[19,30] The planarity of the five-membered ring is confirmed by the values of the torsional angles C4–N1–C7–C8 1.7 (6)° for **5** and C5–N2–C6–C7 3.1(2)° for **7**. Furthermore, in each complex, the two chelating ligands are almost coplanar, as demonstrated by the O–Pt–C_{NOHC}–N torsional angles (O2–Pt01–C4–N2 1.0(5)° for **5** and O2–Pt1–C5–N1 −8.4(2)° for **7**).

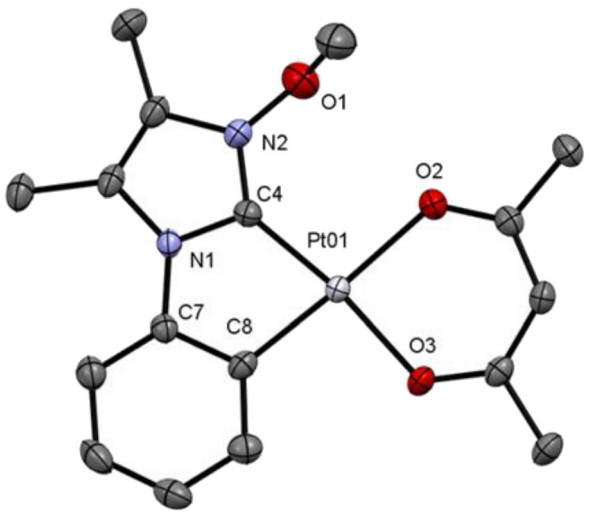

Fig. 2 ORTEP view of complexes **5**. Ellipsoids are drawn at their 50% probability. Hydrogen atoms have been omitted for clarity. Selected bond distances (Å) and angles (°) for **5**: N2–C4 1.334(5), C4–N1 1.369(6), N2–O1 1.382(6), C4–Pt01 1.941(4), C8–Pt01 1.985(5), O2–Pt01 2.081(3), O3–Pt01 2.051(3); C4–Pt01–C8 80.1(2), C4–Pt01–O2 97.0(2), C8–Pt01–O3 92.3(2), O2–Pt01–O3 90.6(1), O2–Pt01–C8 176.9(2), C4–N1–C7–C8 1.7(6), O2–Pt01–C4–N2 1.0(5).

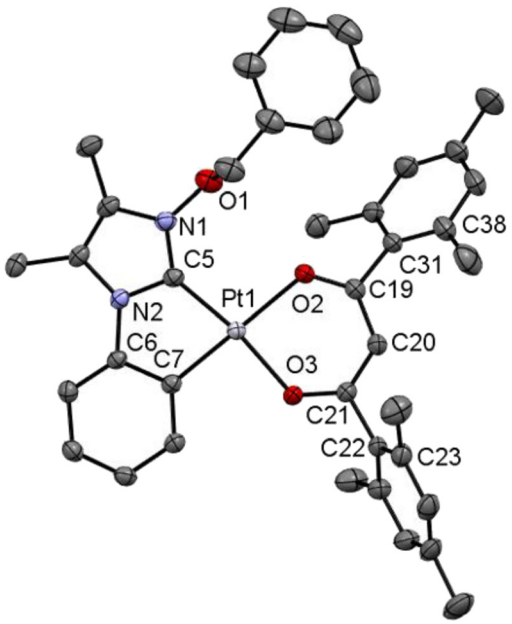

Fig. 3 ORTEP view of complexes **7**. Ellipsoids are drawn at their 50% probability. Hydrogen atoms have been omitted for clarity. Selected bond distances (Å) and angles (°) for **7**: N2–C4 1.400(3), C3–N1 1.395(2), N2–C5 1.365(2), C5–Pt1 1.942(2), C7–Pt1 1.977(2), O2–Pt1 2.102(1), O3–Pt1 2.046(2); C5–Pt1–C7 79.66(7), C5–Pt1–O2 99.57(6), C7–Pt1–O3 91.69(6), O2–Pt1–O3 89.31(6), O2–Pt1–C7 79.66(7), C5–N2–C6–C7 3.1 (2), O2–Pt1–C5–N1 −8.4(2), C20–C21–C22–C23 86.6(2), C20–C19–C31–C38 57.0(3).

Also, the Pt–O and Pt–C bond lengths are in agreement with values reported in the literature for analogous bonds. In complex **7**, mesityl moieties are orthogonal to the plane defined by the β-diketonate auxiliary ligand, as the dihedral angles C20–C21–C22–C23 and C20–C19–C31–C38 are 86.6(2)° and 57.0(3)°, respectively.

No Pt–Pt interaction is present in the crystal packing (*cf.* ESI Fig. S21 and 22†) of the two complexes as the metal centres are not superimposed and their distance is larger than the sum of their van der Waals radii.

Photophysical properties

Absorption spectra of proligand **3** (Fig. S23†) and complexes **5**–**7** (Fig. 4) were measured at room temperature in a 5×10^{-5} M dichloromethane solution.

The absorbance onsets of complexes **5** and **6** are observed at 365 nm while the mesacac complex **7** already absorbs at approximately 390 nm. All three complexes show a relatively strong absorbance band at 320 nm. No significant difference in the absorption maxima wavelength is observed when changing the hydrocarbon moiety bound to the oxygen atom at the NOHC or when changing the auxiliary ligand. These features are similar to the analogous complexes with NHC ligands with simple alkyl groups as nitrogen substituents.[19,30]

The emission spectra were also recorded in a 2 wt% matrix of PMMA (60 μm) on a quartz glass substrate under N_2 atmosphere at room temperature (ESI Fig. S24†). Unfortunately, the

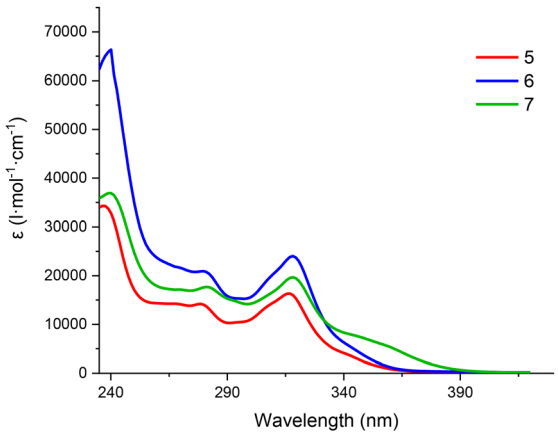

Fig. 4 Absorption spectra of compounds **5–7** recorded in CH_2Cl_2 solutions (5×10^{-5} M) at room temperature. Cuvette length d = 1 cm.

quantum yields were too poor to give accurate photophysical data. Nevertheless, complex **5** and the related compound with the 3,4,5-trimethyl-1-(phenyl-κC^2)-imidazol-2-ylidene ligand[30] exhibit very similar photoluminescence properties, highlighting that the addition of the oxygen in the wingtip substituent does not significantly modify the photophysical parameters of the platinum(II) complexes.

Electrochemistry of the platinum(II) complexes

The electrochemical properties of the platinum(II) complexes were investigated by cyclic voltammetry (Fig. 5) and differential pulse voltammetry. None of the observed events is reversible, which is typical for Pt(II) complexes in their d^8 configuration as every redox event should lead to a significant structural change.

The values of the reduction potential for compounds **5** and **6** are very close (−2.73 and −2.75 V, respectively). The DFT calculations for these complexes support this result as the LUMO

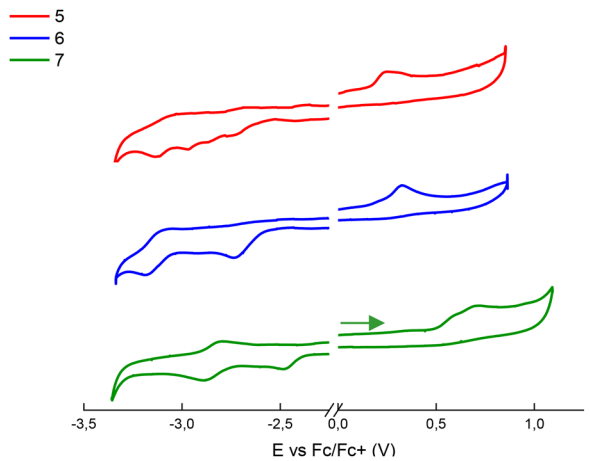

Fig. 5 Cyclic voltammograms of complexes **5–7** in dimethylformamide at 100 mV s^{-1} (c = 0.5 mM), referenced internally against Fc/Fc^+. The green arrow indicates the initial scan direction.

Table 1 Electrochemical properties and calculated HOMO–LUMO energies based on obtained DPV data for complexes **5–7**

	E_{ox} [a] (V)	E_{HOMO} [b] (eV)	E_{Red} [a] (V)	E_{LUMO} [c] (eV)	E_g [d] (eV)
5	0.25	−4.95	−2.73	−1.53	3.42
6	0.32	−5.05	−2.75	−1.51	3.54
7	0.61	−5.59	−2.48	−1.83	3.76

[a] Redox potentials, referenced internally *vs.* Fc/Fc^+. [b] Calculated HOMO energies, E_{HOMO} [eV] = $-1.4 \times E_{ox} - 4.6$ V.[33] [c] Calculated LUMO energies, E_{LUMO} [eV] = $-1.19 \times E_{red} - 4.78$ V.[34] [d] Calculated band gap, $E_g = |E_{HOMO} - E_{LUMO}|$.

is mostly located on the acac ligand, and it is almost identical for the two species (*vide infra*) (*cf.* ESI Fig. S31†). As displayed for similar complexes, the substitution of the acac with the mesacac ligand (complexes **6** and **7**, respectively) leads to a positive shift of both the oxidation and reduction potential.[21] Energies for the HOMO and LUMOs of all three Pt(II) complexes are summarized in Table 1.

Based on the respective differential pulse voltammograms (*cf.* ESI Fig. S26, S28 and S30†), HOMO–LUMO gaps (E_g) between 3.42 V and 3.76 V could be determined. As mentioned before, the energy levels of the HOMO and LUMO in complex **7** vary compared to the [(C_{NOHC}^C*)Pt(acac)] species **5** and **6**, which was also found in earlier studies.[18,19]

Quantum chemistry

Density functional theory (DFT) calculations with the PBE0 functional and 6-311G* basis set were employed in order to

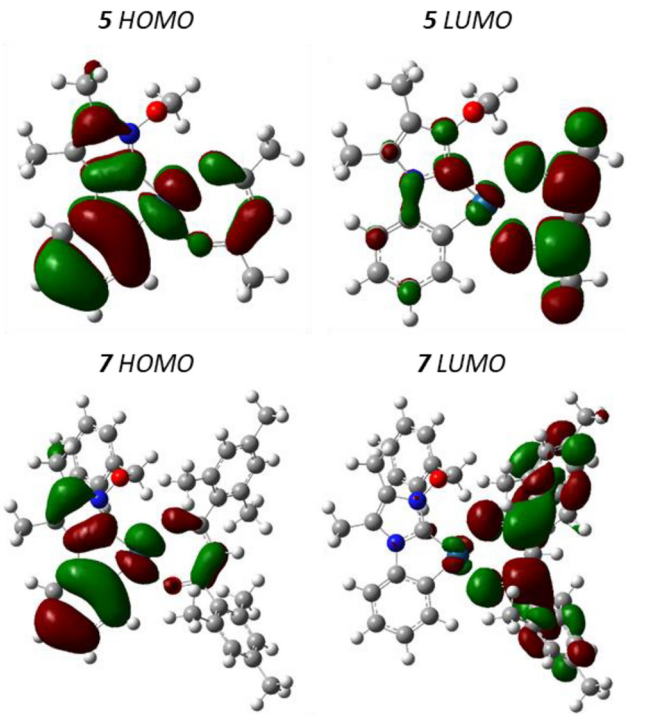

Fig. 6 Frontier molecular orbitals HOMO and LUMO of compounds **5** and **7** (isovalue = 0.03).

optimize the geometries of the Pt(II) complexes in the ground state, confirming them as true minima by the absence of negative eigenvalues in the vibrational frequency analysis. Platinum was treated by an LANL2TZ ECP (*cf.* ESI† for computational details). The ground state geometries are in good agreement with the obtained crystal structures. Furthermore, HOMO and LUMO plots (Fig. 6 for **5** and **7**) (ESI Fig. S31† for **6**) were generated and visualized for analysis of the electronic structure of complexes **5–7**. In general, the HOMO of all three platinum(II) complexes is distributed over the π-system of the C_{NOHC}^C* ligand and the d-orbitals of the Pt(II) centre with little contribution of bonding π-orbitals of the 1,3-diketonate. No orbital contribution is exerted by the oxygen atom of the NOHC. The LUMO is localized over the entire β-diketonate, including the mesityl rings of complex **7**, which supports the observed difference of the LUMO energies retrieved from the CV investigations (*vide supra*).

Conclusions

Two precursors of NOHC ligands, **2** and **3**, characterized by a different group on the oxygen atom (Me or Bn respectively) were synthesized. With the proligand with benzyl substituent the gold(I) complex **4** was obtained, while starting with both proligands three C_{NOHC}^C* platinum(II) complexes, **5–7**, could be isolated with β-diketonate auxiliary ligands. To the best of our knowledge, they are the first Pt(II)-NOHC compounds reported and characterized in the literature. The structures of **4**, **5** and **7** were also solved with X-ray diffraction analysis. Additionally, the absorption, luminescence and electrochemical behaviour of the novel platinum species were investigated which revealed a predominant role of the auxiliary β-diketonate ligand over the C_{NOHC}^C* ligand. These findings were further emphasized by DFT calculations at the triple-ζ level of theory.

Experimental section

All manipulations were carried out using standard Schlenk techniques and all the reactants were obtained from commercial suppliers and used as received. Solvents were dried over molecular sieves or distilled before use. 3-(hydroxyimino) butan-2-one[35] and hexahydro-1,3,5-triphenyltriazine[36] were prepared according to literature procedures. General information about instrumentation, solid-state structure determination, and computational methods can be found in the ESI.†

Synthesis of 1-phenylimidazolium-3-oxide 1

3-(hydroxyimino)butan-2-one (3.95 g, 39.1 mmol) was stirred with hexahydro-1,3,5-triphenyltriazine (4.10 g, 13.0 mmol) in glacial acetic acid (20 ml) for 40 h at room temperature in a two-necked round-bottom flask. The yellow solution changed its colour to orange after 40 h. Then, gaseous HCl was bubbled into the solution for 2 h at room temperature. Diethyl ether (200 ml) was added until a white precipitate appeared. The mixture was kept at 4 °C overnight. The solid was filtered, washed with diethyl ether (4 × 50 ml) and dissolved in a mixture of $CHCl_3$/MeOH (5 : 1, 30 ml). Na_2CO_3 (1.90 g) was added in excess to the solution, which was then stirred for 30 minutes. The remaining solid was filtered off and the solvent evaporated to dryness. The obtained solid was purified by column chromatography (EtOAc/MeOH 1 : 1 to 1 : 2), yielding **1** as a white solid. Yield: 3.76 g, 20.0 mmol, 51%. ^{1}H NMR (300 MHz, $CDCl_3$): δ (ppm) = 2.12 (s, CH_3, 3H), 2.30 (s, CH_3, 3H), 7.28–7.33 (m, CH_{arom}, 2H), 7.47–7.58 (m, CH_{arom}, 3H), 8.23 (s, NCHN, 1H). $^{13}C\{^1H\}$ NMR (75 MHz, $CDCl_3$): δ (ppm) = 7.6 (CH_3), 9.6 (CH_3), 122.2 (C_{arom}), 125.7 (CH_{arom}), 126.1 (CH_{arom}), 127.4 (C_{arom}), 129.7 (CH_{arom}), 130.1 (CH_{arom}), 134.8 (C_{arom}). HRMS (TOF, 0.5 mM NH_4OAc): (m/z) $[M + H]^+$ calc.: 189.1022, found: 189.1032. Melting point: 169–173 °C.

Synthesis of 1-phenyl-3-methoxylimidazolium iodide 2

1-Phenylimidazole-3-oxide **1** (0.67 g, 3.56 mmol) and methyl iodide (0.22 ml, 3.56 mmol) were dissolved in anhydrous THF (10 ml) and stirred for 24 h at room temperature in a pressure tube. The reaction was monitored with TLC in MeOH/EtOAc 1 : 1. The reaction was stopped after 24 h when no significant amount of starting material was detected in the reaction mixture. The product was filtered, washed with diethyl ether and dried *in vacuo*. Yield: 0.952 g, 2.9 mmol, 81%. ^{1}H NMR (300 MHz, $CDCl_3$): δ (ppm) = 2.20 (s, 3H, CH_3), 2.42 (s, 3H, CH_3), 4.59 (s, 3H, OCH_3), 7.51–7.61 (m, 3H, CH_{arom}), 7.64–7.72 (m, 2H, CH_{arom}), 10.12 (s, 1H, NCHN). $^{13}C\{^1H\}$ NMR (75 MHz, $CDCl_3$): δ (ppm) = 7.8 (CH_3), 9.8 (CH_3), 70.5 (OCH_3), 125.0 (C_{arom}), 126.0 (C_{arom}), 126.6 (CH_{arom}), 130.4 (CH_{arom}), 130.8 (CH_{arom}), 131.2 (CH_{arom}), 132.9 (C_{arom}). HRMS (TOF, 0.5 mM NH_4OAc): (m/z) $[M - OCH_3]^+$ calc.: 172.1000, found: 172.0999; $[M]^+$ calc.: 203.1179, found: 203.1189. Melting point: 122–126 °C.

Synthesis of 1-phenyl-3-benzyloxylimidazolium bromide 3

1-Phenylimidazole-3-oxide **1** (0.50 g, 2.66 mmol) and benzyl bromide (0.32 ml, 2.66 mmol) were dissolved in anhydrous THF (10 ml) and stirred for 6 days at room temperature in a pressure tube. The beige solid was filtrated and washed with diethyl ether. Yield: 0.59 g, 1.64 mmol, 61%. ^{1}H NMR (300 MHz, $CDCl_3$): δ (ppm) = 2.11 (s, 3H, CH_3), 2.13 (s, 3H, CH_3), 5.89 (s, 2H, CH_2), 7.35–7.44 (m, 3H, CH_{arom}), 7.52–7.59 (m, 3H, CH_{arom}), 7.60–7.69 (m, 4H, CH_{arom}), 10.65 (s, 1H, NCHN). $^{13}C\{^1H\}$ NMR (75 MHz, $CDCl_3$): δ (ppm) = 7.6 (CH_3), 9.6 (CH_3), 84.5 (OCH_2), 124.7 (C_{arom}), 125.4 (C_{arom}), 126.3 (CH_{arom}), 129.1 (CH_{arom}), 130.3 (CH_{arom}), 130.5 (CH_{arom}), 131.0 (CH_{arom}), 131.1 (CH_{arom}), 132.4 (C_{arom}), 132.6 (CH_{arom}), 133.0 (C_{arom}). HRMS (TOF, 0.5 mM NH_4OAc): (m/z) $[M]^+$ calc.: 279.1492, found: 279.1497. Melting point: 123–127 °C.

Synthesis of the gold complex 4

1-Phenyl-3-benzyloxyimidazolium bromide **3** (72 mg, 0.20 mmol) was stirred with $Au(SMe_2)Cl$ (59 mg, 0.20 mmol) and K_2CO_3 (276 mg, 2.0 mmol) in acetonitrile (40 ml) at room

temperature under inert atmosphere in a 250 ml two-necked round bottom flask for 48 h. Although the ^{1}H NMR of reaction mixture withdrawal detected the presence of some residual proligand (5 : 2 complex : proligand), the mixture was concentrated to 5 ml and diethyl ether (30 ml) was added. After storing the mixture at 4 °C only crystals of complex **4** formed. Yield: 32 mg, 0.06 mmol, 30%. ^{1}H NMR (300 MHz, CD_3CN): δ (ppm) = 1.95 (s, 6H, CH_3), 5.44 (s, 2H, CH_2), 7.40–7.53 (m, 5H, CH_{arom}), 7.54–7.64 (m, 5H, CH_{arom}). ^{13}C{^{1}H} NMR (75 MHz, CD_3CN): δ (ppm) = 8.0 (CH_3), 10.0 (CH_3), 83.4 (OCH_2), 124.1, 125.1, 128.5, 128.6, 129.9, 130.6, 130.8, 131.4, 131.5, 134.3, 139.1, 167.3 (Au–C). HRMS (TOF, CH_3CN): (m/z) $[L_2Au]^+$ calc.: 753.2499, found: 753.2494. Melting point: 172–175 °C.

Synthesis of the platinum complexes 5 and 6

In a flame-dried Schlenk tube, **2** or **3** (0.80 mmol) and silver(I) oxide (0.40 mmol) were stirred overnight at room temperature in anhydrous dimethylformamide. Dichloro(1,5-cyclooctadiene)platinum(II) (0.80 mmol) was then added in argon counterflow. The mixture was stirred for 24 h at room temperature and overnight at 120 °C. Na(acac) (1.60 mmol) was then added in argon counterflow and the mixture was stirred at 110 °C for 5 h and finally cooled down to room temperature. The solvent was evaporated in high vacuum under mild heating. The black crude solid was extracted with dichloromethane and the mixture filtered through a Celite pad. The red-purple liquid was evaporated under vacuum (rotary evaporator) to give a residue that was purified as specified below.

Complex 5. The crude solid was purified through a chromatographic column with pure dichloromethane as eluent (R_f = 0.5). A yellow solid was isolated and washed with diethyl ether and pentane. Yield: 95.0 mg, 0.20 mmol, 24%. ^{1}H NMR (300 MHz, CD_2Cl_2): δ (ppm) = 1.99 (s, 3H, CH_3), 2.02 (s, 3H, CH_3), 2.17 (s, 3H, CH_3), 2.49 (s, 3H, CH_3), 4.14 (s, 3H, OCH_3), 5.52 (s, 1H, CH_{acac}), 6.87–7.03 (m, 2H,crus CH_{arom}), 7.11–7.26 (m, 1H, CH_{arom}), 7.58–7.85 (m, 1H, CH_{arom}). ^{13}C{^{1}H} NMR (151 MHz, CD_2Cl_2): δ (ppm) = 7.1 (CH_3), 11.2 (CH_3), 27.9 (CH_3), 28.1 (CH_3), 67.3 (OCH_3), 102.1 (CH_{acac}), 112.5 (CH_{arom}), 120.8 (C_{arom}), 121.5 (C_{arom}), 123.7 (CH_{arom}), 126.0 (C_{arom}), 131.9 (CH_{arom}), 144.4 (NCN), 149.6 (C_{arom}), 184.8 (C–O_{acac}), 186.1 (C–O_{acac}). ^{195}Pt NMR (129 MHz, CD_2Cl_2): δ (ppm) = −3450.8. HRMS (TOF, 0.5 mM NH_4OAc): (m/z) $[M + H]^+$ calc.: 496.1194 found: 496.1204. Melting point: 214–218 °C.

Complex 6. The crude product was purified through two chromatographic columns (1 : 1 CH_2Cl_2/isohexane R_f = 0.3 and then 3 : 2 CH_2Cl_2/isohexane R_f = 0.4). A white solid was obtained after removal of the solvents. The solid was washed with isohexane and finally dried in the Schlenk line. Yield: 38.3 mg, 0.07 mmol, 6%. ^{1}H NMR (300 MHz, CD_2Cl_2): δ (ppm) = 1.75 (s, 3H, CH_3), 1.85 (s, 3H, CH_3), 2.03 (s, 3H, CH_3), 2.43 (s, 3H, CH_3), 5.43 (s, 2H, CH_2), 5.51 (s, 1H, CH_{acac}), 6.88–7.04 (m, 2H, CH_{arom}), 7.13–7.25 (m, 1H, CH_{arom}), 7.33–7.46 (m, 5H, CH_{arom}), 7.61–7.89 (m, 1H, CH_{arom}). ^{13}C{^{1}H} NMR (151 MHz, CD_2Cl_2): δ (ppm) = 8.9 (CH_3), 12.8 (CH_3), 29.5 (CH_3), 29.7 (CH_3), 83.5 (OCH_2), 103.8 (CH_{acac}), 114.1 (CH_{arom}), 122.0 (C_{arom}), 124.1 (C_{arom}), 125.3 (CH_{arom}), 125.4 (CH_{arom}), 127.5 (C_{arom}), 130.5 (CH_{arom}), 130.9 (CH_{arom}), 131.4 (CH_{arom}), 133.4 (CH_{arom}), 136.5 (C_{arom}), 146.0 (NCN), 151.2 (C_{arom}), 186.4 (C–O_{acac}), 187.9 (C–O_{acac}). ^{195}Pt NMR (129 MHz, CD_2Cl_2): δ (ppm) = −3454.3. HRMS (TOF, 0.5 mM NH_4OAc): (m/z) $[M + Na]^+$ calc.: 594.1327, found 594.1332. Melting point: 153–157 °C.

Synthesis of platinum complex 7

In a flame-dried Schlenk tube, **3** (431 mg, 1.20 mmol) and silver(I) oxide (167 mg 0.72 mmol) were stirred overnight at room temperature in anhydrous dimethylformamide. Dichloro (1,5-cyclooctadiene)platinum(II) (449 mg, 1.20 mmol) was added in argon counterflow. The mixture was stirred for 24 h at room temperature and overnight at 120 °C. Dry potassium *tert*-butoxide (269 mg, 2.40 mmol) and 1,3-bis(2,4,6-trimethylphenyl)propane-1,3-dione (740 mg, 2.40 mmol) were added in argon counterflow. The mixture was stirred at 110 °C for 5 h, then cooled down to room temperature. The solvent was evaporated in high vacuum (Schlenk line) under mild heating. The black residue was extracted with dichloromethane and filtered through a Celite pad. The dark red liquid was evaporated under vacuum (rotary evaporator) to give a residue that was purified through a chromatographic column with CH_2Cl_2/isohexane 1 : 2 as eluent (R_f = 0.2). A second column was performed to separate the free Hmesacac (from 1 : 3 CH_2Cl_2/isohexane to 1 : 2 CH_2Cl_2/isohexane). The solid was washed with distilled pentane and sonicated twice before drying in the Schlenk line. Yield: 80.4 mg, 0.10 mmol, 9%. ^{1}H NMR (300 MHz, CD_2Cl_2): δ (ppm) = 1.93 (s, 3H, CH_3), 2.27–2.38 (m, 18H, CH_3 mesacac), 2.47 (s, 3H, CH_3), 5.22 (s, 2H, OCH_2), 5.66 (s, 1H, $CH_{mesacac}$), 6.77–7.12 (m, 10H, CH_{arom}), 7.15–7.31 (m, 2H, CH_{arom}), 7.49–7.77 (m, 1H, CH_{arom}). ^{13}C{^{1}H} NMR (151 MHz, CD_2Cl_2): δ (ppm) = 7.6 (CH_3), 11.3 (CH_3), 19.7 (CH_3), 20.0 (CH_3), 21.2 (CH_3), 82.1 (OCH_2), 107.5 ($CH_{mesacac}$), 112.6 (CH_{arom}), 120.7 (C_{arom}), 122.2 (C_{arom}), 123.8 (CH_{arom}), 123.9 (CH_{arom}), 125.8 (C_{arom}), 128.5 (CH_{arom}), 128.6 (CH_{arom}), 128.7 (CH_{arom}), 129.1 (CH_{arom}), 130.2 (CH_{arom}), 132.0 (CH_{arom}), 134.0 (C_{arom}), 134.2 (C_{arom}), 134.4 (C_{arom}), 137.9 (C_{arom}), 138.1 (C_{arom}), 139.6 (C_{arom}), 140.3 (C_{arom}), 144.2 (NCN), 149.6 (C_{arom}), 184.3 (C–$O_{mesacac}$), 186.6 (C–$O_{mesacac}$). ^{195}Pt NMR (129 MHz, CD_2Cl_2): δ (ppm) = −3398.1. HRMS (TOF, 0.5 mM NH_4OAc): (m/z) $[M + H]^+$ calc.: 780.2759, found: 780.2770. Melting point: 148–152 °C.

Author contributions

A. B.: investigation, visualization; J. I. K.: investigation, writing-review & editing; T. R.: investigation, writing-review & editing; F. W.: investigation, writing-review & editing; C. G.: investigation, writing-review & editing; T. S.: conceptualization, funding acquisition, project administration, resources, supervision, writing-original draft, writing-review & editing; C. T.: conceptualization, resources, supervision, writing-original draft, writing-review & editing.

Conflicts of interest

There are no conflicts to declare.

Acknowledgements

We thank the ZIH Dresden for allocating computational time on their high-performance computing facility.

References

1 A. J. I. Arduengo, R. L. Harlow and M. Kline, *J. Am. Chem. Soc.*, 1991, **113**, 361–363.
2 H. V. Huynh, *The Organometallic Chemistry of N-Heterocyclic Carbenes*, John Wiley & Sons, Inc., Hoboken, NJ, 2017.
3 S. P. Nolan, *N-Heterocyclic Carbenes, Effective Tools for Organometallic Synthesis*, Wiley-VCH, Weinheim, 2014.
4 S. Diez-Gonzalez, *N-Heterocyclic Carbenes: From Laboratory Curiosities to Efficient Synthetic Tools*, RSC Catalysis Series, RSC, Cambridge, 2nd edn, 2017.
5 C. A. Smith, M. R. Narouz, P. A. Lummis, I. Singh, A. Nazemi, C.-H. Li and C. M. Crudden, *Chem. Rev.*, 2019, **119**, 4986–5056.
6 S. Ibáñez, M. Poyatos and E. Peris, *Acc. Chem. Res.*, 2020, **53**, 1401–1413.
7 A. T. Biju, *N-Heterocyclic Carbenes in Organocatalysis*, Wiley-VCH, Weinheim, 2018.
8 G. Laus, K. Wurst, V. Kahlenberg, H. Kopacka, C. Kreutz and H. Schottenberger, *Z. Naturforsch., B: Chem. Sci.*, 2010, **65**, 776–782.
9 G. Laus, A. Schwärzler, P. Schuster, G. Bentivoglio, M. Hummel, K. Wurst, V. Kahlenberg, T. Lörting, J. Schütz, P. Peringer, G. Bonn, G. Nauer and H. Schottenberger, *Z. Naturforsch., B: Chem. Sci.*, 2007, **62**, 295–308.
10 A. Wróblewska, G. Lauriol, G. Mlostoń, X. Bantreil and F. Lamaty, *J. Organomet. Chem.*, 2021, **949**, 121914.
11 V. V. Bakhonsky, J. Becker, G. Mlostoń and P. R. Schreiner, *Chem. Commun.*, 2022, **58**, 1538–1541.
12 M. Alcarazo, R. Fernández, E. Álvarez and J. M. Lassaletta, *J. Organomet. Chem.*, 2005, **690**, 5979–5988.
13 F. J. Gómez, N. E. Kamber, N. M. Deschamps, A. P. Cole, P. A. Wender and R. M. Waymouth, *Organometallics*, 2007, **26**, 4541–4545.
14 B. Rietzler, G. Laus, V. Kahlenberg and H. Schottenberger, *Acta Crystallogr., Sect. E: Crystallogr. Commun.*, 2015, **71**, m251–m252.
15 G. Mlostoń, M. Celeda, M. Jasiński, K. Urbaniak, P. J. Boratyński, P. R. Schreiner and H. Heimgartner, *Molecules*, 2019, **24**, 4398.
16 G. Mlostoń, M. Celeda, K. Urbaniak, M. Jasiński, V. Bakhonsky, P. R. Schreiner and H. Heimgartner, *Beilstein J. Org. Chem.*, 2019, **15**, 497–505.
17 C. Lin, C. Xia and J.-Y. Tsai, Organic Electroluminescent materials and devices, *European Patent*, EP2891659B1, 2015.
18 S. Stipurin and T. Strassner, *Inorg. Chem.*, 2021, **60**, 11200–11205.
19 S. Stipurin and T. Strassner, *Eur. J. Inorg. Chem.*, 2021, **2021**, 804–813.
20 S. Stipurin and T. Strassner, *Eur. J. Inorg. Chem.*, 2022, **2022**, e202200295.
21 S. Stipurin, F. Wurl and T. Strassner, *Organometallics*, 2022, **41**, 313–320.
22 T. Riesebeck and T. Strassner, *Organometallics*, 2023, **42**, 3275–3282.
23 P. Pinter, J. Soellner and T. Strassner, *Eur. J. Inorg. Chem.*, 2021, **2021**, 3104–3107.
24 J. Soellner, P. Pinter, S. Stipurin and T. Strassner, *Angew. Chem., Int. Ed.*, 2021, **60**, 3556–3560.
25 A. Tronnier, U. Heinemeyer, S. Metz, G. Wagenblast, I. Muenster and T. Strassner, *J. Mater. Chem. C*, 2015, **3**, 1680–1693.
26 T. Scattolin and S. P. Nolan, *Trends Chem.*, 2020, **2**, 721–736.
27 E. A. Martynova, N. V. Tzouras, G. Pisanò, C. S. J. Cazin and S. P. Nolan, *Chem. Commun.*, 2021, **57**, 3836–3856.
28 S. K. Goetzfried, C. M. Gallati, M. Cziferszky, R. A. Talmazan, K. Wurst, K. R. Liedl, M. Podewitz and R. Gust, *Inorg. Chem.*, 2020, **59**, 15312–15323.
29 C. Schmidt, L. Albrecht, S. Balasupramaniam, R. Misgeld, B. Karge, M. Brönstrup, A. Prokop, K. Baumann, S. Reichl and I. Ott, *Metallomics*, 2019, **11**, 533–545.
30 S. Stipurin and T. Strassner, *J. Organomet. Chem.*, 2023, **1000**, 122785.
31 Y. Unger, D. Meyer, O. Molt, C. Schildknecht, I. Münster, G. Wagenblast and T. Strassner, *Angew. Chem., Int. Ed.*, 2010, **49**, 10214–10216.
32 B. L. Eriksen, P. Vedsø, S. Morel and M. Begtrup, *J. Org. Chem.*, 1998, **63**, 12–16.
33 B. W. D'Andrade, S. Datta, S. R. Forrest, P. Djurovich, E. Polikarpov and M. E. Thompson, *Org. Electron.*, 2005, **6**, 11–20.
34 P. I. Djurovich, E. I. Mayo, S. R. Forrest and M. E. Thompson, *Org. Electron.*, 2009, **10**, 515–520.
35 R. U. Gutiérrez, A. Rebollar, R. Bautista, V. Pelayo, J. L. Várgas, M. M. Montenegro, C. Espinoza-Hicks, F. Ayala, P. M. Bernal, C. Carrasco, L. G. Zepeda, F. Delgado and J. Tamariz, *Tetrahedron: Asymmetry*, 2015, **26**, 230–246.
36 A. G. Giumanini, G. Verardo, E. Zangrando and L. Lassiani, *J. Prakt. Chem.*, 1987, **329**, 1087–1103.